Proceedings of IMECE2005
2005 ASME International Mechanical Engineering Congress and Exposition
November 5-11, 2005, Orlando, Florida USA

IMECE2005-79582

MODEL-FREE TRAJECTORY CONTROL OF A TWO-LINK FLEXIBLE-JOINT ROBOT: THEORY AND EXPERIMENT

Withit Chatlatanagulchai
Motion and Vibration Control Laboratory,
School of Mechanical Engineering,
Purdue University. (e-mail: chatlata@purdue.edu).

Peter H. Meckl
Motion and Vibration Control Laboratory,
School of Mechanical Engineering,
Purdue University. (e-mail: meckl@purdue.edu;
phone: 765-494-0539; fax: 765-494-5686).

ABSTRACT

We present a state-feedback control of a two-link flexible-joint robot. First, we obtain desired control laws from Lyapunov's second method. Then, we use three-layer neural networks to learn the unknown parts of the desired control laws. In this way, the control algorithm does not require the mathematical model representing the robot. We use a smooth variable structure controller to handle uncertainties from the neural network approximation and external disturbances. To show the effectiveness and practicality of this control algorithm, we performed an experiment on one of the robots in our laboratory.

Keywords: Flexible-joint robot, Intelligent control, Backstepping, Variable structure control.

1. INTRODUCTION

We are interested in motion control of a flexible-joint robot for several reasons. First, the joint flexibility exists in most robots. It arises from driving components such as actuators, gear teeth, or transmission belts. In some applications, the designers incorporate flexible joints into their products intentionally to absorb impact force and to reduce damage to the parts from accidental collision. Second, control designers should explicitly include joint flexibility in their design because joint resonant frequencies, which are located within the control bandwidth, can be excited and cause severe oscillations. The experiment in [1] suggested that the designers should consider joint flexibility in both modeling and control design.

Controller design of two-link flexible-joint robot is challenging due to two main reasons. First, its Euler-Lagrange model is much more complicated than those of rigid-joint or one-link flexible-joint robot. Second, the number of degrees of freedom is twice the number of control inputs. The control inputs do not directly apply to the links. Instead, the control inputs directly apply to the motors that connect to the links via flexible-joint dynamics. This results in the loss of some important structural properties that apply for rigid-joint robots, such as matching property between nonlinearities and the inputs, passivity from inputs to link velocities.

There exist some well-established control designs for flexible-joint robots. In [2], they transform the dynamic model of the flexible-joint robot into the standard singular perturbation model, by using link position as slow variable and joint torque as fast variable. Controller is a composite of slow and fast control. Slow-control input, which adds damping to the system, drives the closed-loop system to a quasi-steady state system that has the structure of a rigid-joint robot. Then, fast-control input can be designed using available techniques for the rigid-joint robot. To avoid having to measure the joint torque signal, you may consult [3] for the design of an observer. Reference [4] shows an alternative singular perturbation model by using tracking error of motor shaft as fast variable. Reference [5] extends the work in [2] to the case where model uncertainties exist in the system. They use radial basis function networks to estimate unknown functions, and use discontinuous variable-structure controller to provide the closed-loop system with robustness for the estimation errors.

Under the assumption that the kinetic energy of the motor is due mainly to its own rotation, the flexible-joint robot model is feedback linearizable by static feedback control laws as in [6]. Reference [7] relaxes this assumption, and applies the so-called dynamic feedback linearization method to a more general robot model.

Reference [8] compares three types of controllers: controller developed from decoupled model, backstepping controller, and passivity-based controller. For the first type, they interestingly decouple the robot model by using filtered error of link position and motor position error as variables. They also discuss backstepping controller when model parameters are unknown but can be made to appear linearly with respect to known functions. Passivity-based controller is designed to shape the closed-loop total energy to desired value to achieve passivity.

Some of the more recent work are [9]-[12]. Reference [9] has experimental result on one-link flexible-joint robot in vertical plane. Reference [10] uses feedback linearization method and Takagi-Sugeno fuzzy system to replace model uncertainties. Reference [11] contains good references on flexible-joint and flexible-link robots. Reference [12] is written from practitioner's point of view.

This paper has the following features:

1) We consider a trajectory-tracking task of a two-link flexible-joint robot in the horizontal plane. The second motor is attached to the first link and its shaft does not share the same axis with the axis of rotation of the second link. This setting is more practical than the shared-axis cases commonly treated in the existing literature.

2) The controller algorithm does not require a closed-form mathematical model of the robot. We design control laws from Lyapunov's second method using backstepping structure. Then, three-layer neural networks are used to estimate the unknown parts of the desired control laws – usually called direct method by adaptive control community. We use variable structure controller to provide robustness to the system against uncertainties from the estimation errors, actuator nonlinearities, and external disturbances.

3) We are able to control the trajectory of the robot effectively using link angular position, link angular velocity, motor angular position, and motor angular velocity. Existing work usually requires, in addition to the quantities above, link angular acceleration and jerk, or flexible-joint torque.

Throughout this paper, unless otherwise specified, we have the following definition.

Definition 1: We denote by $\|\bullet\|$ any suitable norm. When it is required to be specific, we denote any p-norm by $\|\bullet\|_P$. The symbol $\|\bullet\|_F$ denotes the Frobenius norm, i.e. given a matrix A, the Frobenius norm is given by $\|A\|_F^2 = tr\left(A^T A\right) = \sum_{ij} a_{ij}^2$.

We organize this paper as follows. Section 2 contains details on the robot and the experimental setup. Section 3 contains three-layer neural network background. Section 4 contains controller design. Section 5 contains experimental results. Section 6 is a conclusion of the paper.

2. A TWO-LINK FLEXIBLE-JOINT ROBOT

Fig. 1 depicts a robot, for which we are designing the controller. The robot operates in the horizontal plane, has two links and two motors. Input torque u_1 is applied to the first motor, which drives the first sprocket through a chain. The sprocket is attached to the first link via the first torsional spring that provides joint flexibility. The second motor is situated on the first link. Input torque u_2 is applied to the second motor which drives the second sprocket. The second sprocket is attached to the second link via the second torsional spring. Note that the second motor's shaft does not share the same axis with the axis of rotation of the second link. This setting is more practical than the shared-axis cases commonly treated in existing literature.

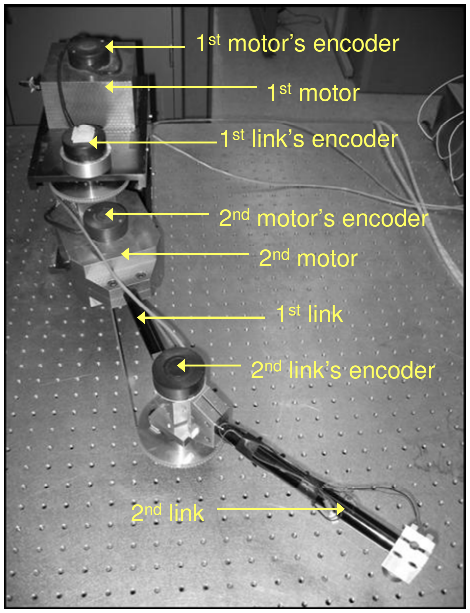

Fig. 1. Photograph of the two-link flexible-joint robot in our laboratory.

There are four optical encoders; each measures angular positions of the two links and the two motors. Angular velocities are obtained from the Euler method

$$\dot{\theta}_i(k+1) = \frac{\theta_i(k+1) - \theta_i(k)}{ts},$$

where ts is sampling period. Two current amplifiers supply current to the two motors.

Fig. 2 depicts the overall experimental setup. We use Labview 7.1, Labview Real-Time Module, and Labview FPGA Module to perform hardware-in-the-loop experiment. The data acquisition board is National Instruments' PCI-7831R.

The controller algorithm presented in this paper does not explicitly require the plant functions. However, to be able to design a controller to maintain closed-loop stability, we need to assume that the actual plant model can be put in the form:

$$\dot{x}_i = f_i(\bar{x}_m) + g_i(\bar{x}_m) x_{i+1}, 1 \le i \le m-1,$$
$$\dot{x}_m = f_m(\bar{x}_m) + g_m(\bar{x}_m) u,$$
$$y = x_1, \tag{1}$$

where $u = [u_1, \ldots, u_n]^T \in \mathbb{R}^n$ represents input to the system,

$x_i = [x_{i1}, \ldots, x_{in}]^T \in \mathbb{R}^n$ represents state subvector, $y = [y_1, \ldots, y_n]^T \in \mathbb{R}^n$ is system output, $\bar{x}_m$ denotes the set $\{x_1, \ldots, x_m\}$, and $f_i \in \mathbb{R}^n$, $g_i \in \mathbb{R}^{n\times n}$, are vector and matrix of unknown smooth functions that may depend on all states.

Next, we will show that the equations of motion of our robot, under an assumption, can be transformed into the form above.

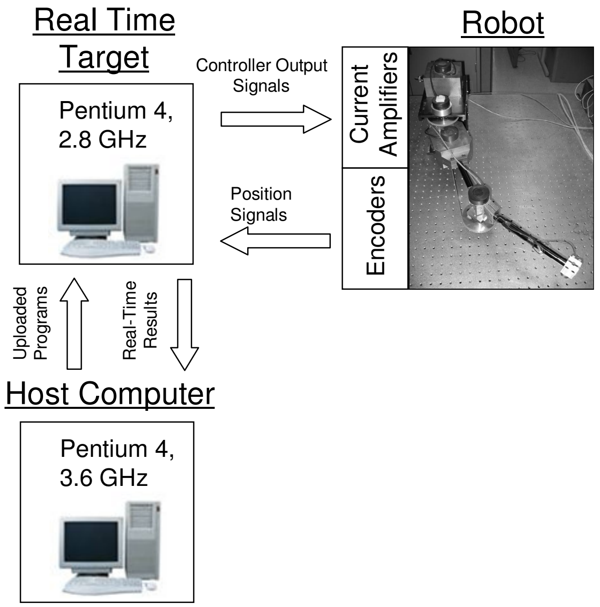

Fig. 2. Diagram showing overall experimental setup.

Consider the schematic diagram of a two-link flexible-joint robot in Fig. 3. Table I contains the description of parameters of the robot.

TABLE I

DESCRIPTION OF PARAMETERS USED IN THE MODELING OF THE TWO-LINK FLEXIBLE-JOINT ROBOT

1st Link	θ_1 : Absolute angular position m_1 : Lumped mass J_1 : Moment of inertia about COG a_1 : Distance between COG of the 1st link and the 1st joint b_1 : Distance between the 1st joint and the 2nd motor l_1 : Distance between the 1st joint and the 2nd joint
2nd Link	θ_2 : Relative angular position to θ_1 m_2 : Lumped mass J_2 : Moment of inertia about COG a_2 : Distance between COG of the 2nd link and the 2nd joint l_2 : Distance between the 2nd joint and the end-effector
1st Motor	θ_3 : Absolute angular position m_3 : Lumped mass J_3 : Inertia of the motor about COG c_3 : Coefficient of friction in the bearing of the motor
2nd Motor	θ_4 : Relative angular position to θ_1 m_4 : Lumped mass J_4 : Inertia of the motor about COG c_4 : Coefficient of friction in the bearing of the motor
1st Sprocket	θ_5 : Absolute angular position after gear reduction, θ_3 / r m_5 : Lumped mass J_5 : Moment of inertia about COG c_1 : Coefficient of friction in the bearing of the joint
1st Spring	k_5 : Coefficient of the torsional spring c_5 : Internal damping of the torsional spring
2nd Sprocket	θ_6 : Relative angular position after gear reduction, θ_4 / r m_6 : Lumped mass J_6 : Moment of inertia about COG c_2 : Coefficient of friction in the bearing of the joint
2nd Spring	k_6 : Coefficient of the torsional spring c_6 : Internal damping of the torsional spring
Payload	m_p : Lumped mass J_p : Moment of inertia about COG
Chain	r : Gear ratio

We let θ_1 be absolute angular position of the first link, θ_2 be relative angular position of the second link, θ_3 be absolute angular position of the first motor, and θ_4 be relative angular position of the second motor. We use Euler-Lagrange method to find dynamic equations governing the robot. First, we compute kinetic energy

$$\begin{aligned}K =\; & \frac{1}{2}\left(m_1 a_1^2 + m_2 l_1^2 + m_4 b_1^2 + m_6 l_1^2 + m_p l_1^2 + J_1\right)\dot{\theta}_1^2 \\ & + \frac{1}{2}\left(m_2 a_2^2 + J_2 + m_p l_2^2 + J_p\right)\left(\dot{\theta}_1 + \dot{\theta}_2\right)^2 + \frac{1}{2}\left(J_3 + \frac{J_5}{r^2}\right)\dot{\theta}_3^2 \\ & + \frac{1}{2} J_4\left(\dot{\theta}_1 + \dot{\theta}_4\right)^2 + \frac{1}{2} J_6\left(\frac{\dot{\theta}_4}{r} + \dot{\theta}_1\right)^2 \\ & + l_1\left(m_2 a_2 + m_p l_2\right)\dot{\theta}_1\left(\dot{\theta}_1 + \dot{\theta}_2\right)\cos\left(\theta_2\right).\end{aligned}$$

To be able to transform the robot model into the form (1), we need the following assumption.

Assumption 1: The rotational kinetic energy of the second motor and the second sprocket is mainly due to their own rotation, by neglecting the kinetic energy from the rotation of the first link. In the kinetic energy equation, therefore, the term $0.5J_4\left(\dot{\theta}_1 + \dot{\theta}_4\right)^2$ becomes $0.5J_4\dot{\theta}_4^2{,}_2$ and the term $0.5J_6\left(\dot{\theta}_1 + \dot{\theta}_4 / r\right)^2$ becomes $0.5J_6\left(\dot{\theta}_4 / r\right)^2$.

To have an idea of how significant the dropped terms are, consider, for example, our robot in Fig. 1 with a motor of mass $2\,kg$ and inertia $0.000525\,kg{\bullet}m^2$. $\dot{\theta}_4$ can be approximated by multiplying $\dot{\theta}_1$ by the gear ratio, $r = 5.3$. b_1 equals 0.1. For the second motor, the total kinetic energy, comprising translational kinetic energy and rotational kinetic energy, is given by

$$K_{motor2} = \frac{1}{2} m_4\left(\dot{\theta}_1 b_1\right)^2 + \frac{1}{2} J_4\left(\dot{\theta}_4 + \dot{\theta}_1\right)^2 = 0.001\,795\,\dot{\theta}_4^2.$$

Under Assumption *1*, the total kinetic energy of the second motor is

$$\bar{K}_{motor2} = \frac{1}{2} m_4 \left(\dot{\theta}_1 b_1\right)^2 + \frac{1}{2} J_4 \left(\dot{\theta}_4\right)^2 = 0.001\,686\,\dot{\theta}_4^2.$$

We can see about 6-percent error in our case. The error, however, is smaller with bigger gear ratio.

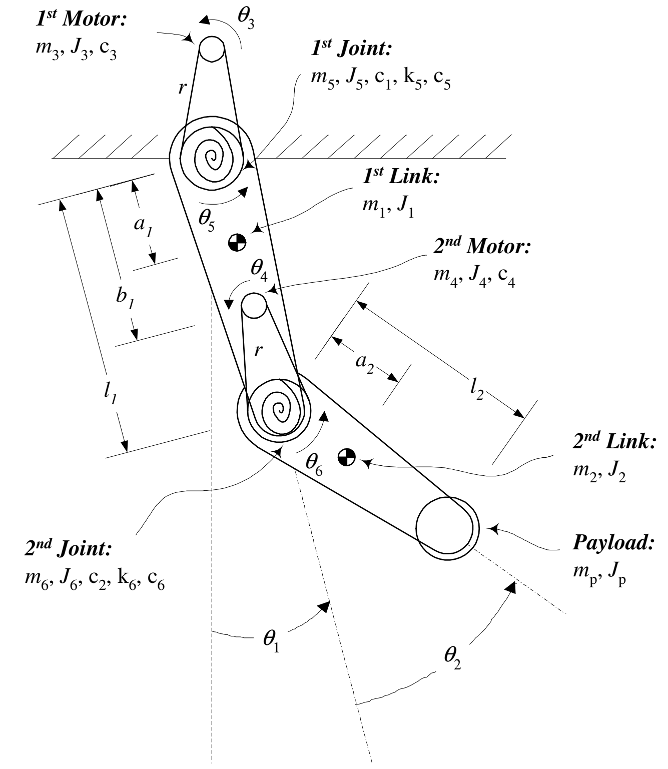

Fig. 3. Schematic diagram of a planar two-link flexible-joint robot.

The potential energy from both torsional springs is

$$P = \frac{1}{2} k_5 \left(\frac{\theta_3}{r} - \theta_1\right)^2 + \frac{1}{2} k_6 \left(\frac{\theta_4}{r} - \theta_2\right)^2.$$

The dissipative power from friction and damping is

$$D = \frac{1}{2} c_3 \dot{\theta}_3^2 + \frac{1}{2} c_1 \dot{\theta}_1^2 + \frac{1}{2} c_5 \left(\frac{\dot{\theta}_3}{r} - \dot{\theta}_1\right)^2 + \frac{1}{2} c_4 \dot{\theta}_4^2 + \frac{1}{2} c_2 \dot{\theta}_2^2 + \frac{1}{2} c_6 \left(\frac{\dot{\theta}_4}{r} - \dot{\theta}_2\right)^2.$$

The work done by input torque is $\delta W = u_1\ \delta\theta_3 + u_2\ \delta\theta_4$. Therefore, the generalized force is

$$Q_1 = 0, Q_2 = 0, Q_3 = u_1, Q_4 = u_2.$$

The Lagrange equations are

$$\frac{d}{dt}\left(\frac{\partial K}{\partial \dot{\theta}_i}\right) - \frac{\partial K}{\partial \theta_i} + \frac{\partial P}{\partial \theta_i} + \frac{\partial D}{\partial \dot{\theta}_i} = Q_i,\ i = 1, 2, 3, 4.$$

With straightforward derivation, we obtain four Lagrange equations from the kinetic energy – revised according to Assumption 1, the potential energy, the dissipative power, and the work done by input torque. Due to the size of the four Lagrange equations, we do not show them here, but instead, we skip to how we obtain the state-space model.

We let $x_1 = \left[x_{11}, x_{12}\right]^T = \left[\theta_1, \theta_2\right]^T$ and $x_2 = \left[x_{21}, x_{22}\right] = \left[\dot{\theta}_1, \dot{\theta}_2\right]^T$ be state vectors representing link position and velocity, $x_3 = \left[x_{31}, x_{32}\right] = \left[\theta_3, \theta_4\right]^T$ and $x_4 = \left[x_{41}, x_{42}\right] = \left[\dot{\theta}_3, \dot{\theta}_4\right]^T$ be state vectors representing motor position and velocity, and $u = \left[u_1, u_2\right]^T$ be input vector representing input torque. The Lagrange equations can be put in the following form

$$\begin{aligned} M\dot{x}_2 + Vx_2 + F_1 + B_1\left(x_2 - x_4\right) + K_1\left(x_1 - x_3\right) = 0, \\ J\dot{x}_4 + F_2 - B_2\left(x_2 - x_4\right) - K_2\left(x_1 - x_3\right) = u. \end{aligned} \tag{2}$$

The inertia matrix is

$$M\left(x_1\right) = \begin{bmatrix} M_{11} & M_{12} \\ M_{21} & M_{22} \end{bmatrix},$$

where

$$\begin{aligned} M_{11} &= m_1 a_1^2 + m_2\left(l_1^2 + a_2^2\right) + m_4 b_1^2 + m_6 l_1^2 + J_1 + J_2 \\ &\quad + m_p\left(l_1^2 + l_2^2\right) + J_p + 2l_1\left(m_2 a_2 + m_p l_2\right)\cos\left(\theta_2\right), \\ M_{12} &= M_{21} = m_2 a_2^2 + J_2 + m_p l_2^2 + J_p \\ &\quad + l_1\left(m_2 a_2 + m_p l_2\right)\cos\left(\theta_2\right), \\ M_{22} &= m_2 a_2^2 + J_2 + m_p l_2^2 + J_p. \end{aligned}$$

$V\left(x_1, x_2\right) x_2$ represents coriolis and centrifugal functions and is given by

$$V\left(x_1, x_2\right) = \begin{bmatrix} 0 & \begin{matrix} -l_1\left(m_2 a_2 + m_p l_2\right) \\ \left(2\dot{\theta}_1 + \dot{\theta}_2\right)\sin\left(\theta_2\right) \end{matrix} \\ \begin{matrix} l_1\left(m_2 a_2 + m_p l_2\right) \\ \dot{\theta}_1 \sin\left(\theta_2\right) \end{matrix} & 0 \end{bmatrix}.$$

K_1, K_2 are joint flexibility matrices

$$K_1 = \begin{bmatrix} k_5 & 0 \\ 0 & k_6 \end{bmatrix}, K_2 = \begin{bmatrix} k_5 / r & 0 \\ 0 & k_6 / r \end{bmatrix}.$$

J represents the inertia of motors and sprockets

$$J = \begin{bmatrix} r\left(J_3 + J_5 / r^2\right) & 0 \\ 0 & r\left(J_4 + J_6 / r^2\right) \end{bmatrix}.$$

B_1, B_2 contain internal damping of the torsional springs

$$B_1 = \begin{bmatrix} c_5 & 0 \\ 0 & c_6 \end{bmatrix}, B_2 = \begin{bmatrix} c_5 / r & 0 \\ 0 & c_6 / r \end{bmatrix}.$$

$F_1\left(x_2\right), F_2\left(x_4\right)$ are viscous friction vectors

$$F_1(x_2)=\begin{bmatrix} c_1\dot{\theta}_1 \\ c_2\dot{\theta}_2 \end{bmatrix},\ F_2(x_4)=\begin{bmatrix} rc_3\dot{\theta}_5 \\ rc_4\dot{\theta}_6 \end{bmatrix}.$$

Suppose, also, that there exists additive disturbance. This disturbance may arise from measurement noise or simply the unmodeled dynamics, e.g., friction in microscopic level. It is reasonable to expect that these disturbances are bounded by some constants; the constants may be unknown.

Let $d_{ai}(\bar{x}_4)=[d_{ai1},d_{ai2}]^T$ be additive disturbance that may depend on all states. We, then, obtain the following state-space model

$$\begin{aligned}
\dot{x}_1 &= x_2 + d_{a1}(\bar{x}_4),\\
\dot{x}_2 &= f_2(\bar{x}_4)+g_2(\bar{x}_4)\left(x_3+d_{a2}(\bar{x}_4)\right),\\
\dot{x}_3 &= x_4 + d_{a3}(\bar{x}_4),\\
\dot{x}_4 &= f_4(\bar{x}_4)+g_4(\bar{x}_4)\left(u+d_{a4}(\bar{x}_4)\right),\\
y &= x_1,
\end{aligned} \tag{3}$$

where

$$f_2=-M^{-1}\left[Vx_2+F_1+B_1(x_2-x_4)+K_1(x_1)\right]=[f_{21},f_{22}]^T,$$

$$g_2=M^{-1}K_1=\begin{bmatrix} g_{211} & g_{212}\\ g_{221} & g_{222}\end{bmatrix},$$

$$f_4=-J^{-1}\left[F_2-B_2(x_2-x_4)-K_2(x_1-x_3)\right]=[f_{41},f_{42}]^T,$$

$$g_4=J^{-1}=\begin{bmatrix} g_{411} & g_{412}\\ g_{421} & g_{422}\end{bmatrix}.$$

In the next section, we will design a controller for the system in the form (3), where f_2, f_4, g_2, and g_4 are unknown. The disturbance d_{ai} is bounded by an unknown constant.

3. THREE-LAYER NEURAL NETWORK

Fig. 4 depicts a three-layer neural network. Suppose, a scalar-valued continuous function $h(z_1,z_2,\ldots,z_n):\mathbb{R}^n\to\mathbb{R}$ is to be estimated by the neural network. We have $z_1,z_2,\ldots,z_n,1$ as inputs to the neural network. Variables in the network are defined as follows:

$$\bar{Z}=[z_1,z_2,\ldots,z_n,1]^T\in\mathbb{R}^{n+1},$$

$$V=[v_1,v_2,\ldots,v_l]\in\mathbb{R}^{(n+1)\times l},$$

$$v_i=\left[v_{i1},v_{i2},\ldots,v_{i(n+1)}\right]^T\in\mathbb{R}^{n+1}, i=1,2,\ldots,l,$$

$$S(V^T\bar{Z})=\left[s(v_1^T\bar{Z}),s(v_2^T\bar{Z}),\ldots,s(v_l^T\bar{Z}),1\right]^T\in\mathbb{R}^{l+1},$$

$$W=[w_1,w_2,\ldots,w_l,w_{l+1}]^T\in\mathbb{R}^{l+1},$$

$$h(W,V,z_1,z_2,\ldots,z_n)=W^TS(V^T\bar{Z})\in\mathbb{R}.$$

$s(\bullet)$ can be any appropriate activation function that is a non-constant, bounded and monotone increasing continuous function. We use a sigmoid function

$$s(x)=1/\left(1+e^{-x}\right), \forall x\in\mathbb{R}.$$

This network can uniformly approximate any scalar-valued continuous function to any arbitrary accuracy with some constant ideal weights W^*,V^*, and some appropriate number of hidden-layer nodes, l^*, as was proved in [13]. From the universal approximation property, we have

$$h(z_1,z_2,\ldots,z_n)=W^{*T}S(V^{*T}\bar{Z})+\varepsilon, \tag{4}$$

where $\|\varepsilon\|<\varepsilon_U$ is approximation error with unknown $\varepsilon_U>0$ provided that $h(\cdot)$ is defined on a compact set Ω_z.

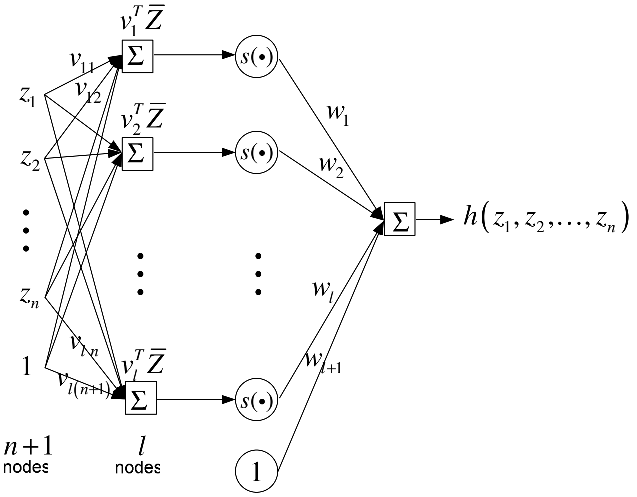

Fig. 4. A three-layer neural network. The square represents node whose output contains adjustable parameters.

Note that the foregoing statement is only to assure the existence of ideal weights and ideal number of hidden-layer nodes. The appropriate number of hidden-layer nodes, in practice, can be found from trial and error with the problem in consideration. The ideal weights generally are unknown. However, in system identification application, the ideal weights are typically assumed constant and bounded as in the following Assumption.

Assumption 2: On the compact set Ω_z, the ideal neural network weights W^*,V^* are constant and bounded by $\|W^*\|\le W_U$, $\|V^*\|_F\le V_U$, $i=1,\ldots,m$, where W_U and V_U are unknown.

Note that the neural network weight V appears nonlinearly. According to [14], approximators that are nonlinear in their parameters can achieve the same level of approximation accuracy as those that are linear and usually require fewer number of adjusting parameters. However, since the parameter appears nonlinearly, the parameter-tuning law is usually more complicated.

Since ideal weights are unknown, let $\hat{W}$ and $\hat{V}$ be the estimates of W^* and V^*, respectively. The estimate of the function h is given by

$$\hat{h}\left(z_1, z_2, \ldots, z_n\right) = \hat{W}^T S\left(\hat{V}^T \bar{Z}\right). \tag{5}$$

By using Lemma 3.6 in [15], the differences between neural network outputs with ideal and estimated weights are given by

$$\begin{aligned}\hat{W}^T S(\hat{V}^T \bar{Z}) - W^{*T} S(V^{*T} \bar{Z}) = \tilde{W}^T (\hat{S} - \hat{S}'\hat{V}^T \bar{Z}) \\ + \hat{W}^T \hat{S}'\tilde{V}^T \bar{Z} + d_u,\end{aligned} \tag{6}$$

where

$$\tilde{W} = \hat{W} - W^*, \tilde{V} = \hat{V} - V^*, \hat{S} = S(\hat{V}^T \bar{Z}) \in \mathbb{R}^{l+1},$$

$$\hat{S}' = diag\left\{\hat{s}_1', \hat{s}_2', \ldots, \hat{s}_l', 0\right\} \in \mathbb{R}^{(l+1)\times(l+1)},$$

$$\hat{s}_i' = s'(\hat{v}_i^T \bar{Z}) = d[s(z_a)]/dz_a\big|_{z_a = \hat{v}_i^T \bar{z}} \in \mathbb{R}, i = 1, 2, \ldots, l,$$

$$s(x) = 1/(1 + e^{-x}), \forall x \in \mathbb{R}.$$

The residual term d_u is bounded by

$$|d_u| \le \|V^*\|_F \left\|\bar{Z}\hat{W}^T \hat{S}'\right\|_F + \|W^*\| \left\|\hat{S}'\hat{V}^T \bar{Z}\right\| + |W^*|_1. \tag{7}$$

Note that $\tilde{W}$ and $\tilde{V}$ appear linearly in (6). This is important since from Assumption 2, $\dot{\tilde{W}} = \dot{\hat{W}}$ and $\dot{\tilde{V}} = \dot{\hat{V}}$, therefore the weight adaptation laws can be easily designed using this linear structure.

4. BACKSTEPPING AND VARIABLE STRUCTURE CONTROLLER

In this section, we design a controller that makes link angular positions θ_1 and θ_2 track desired values whereas all closed-loop signals remain bounded. We require the following assumptions.

Assumption 3: The additive disturbance $d_{aik}\left(\bar{x}_4\right)$, where $i = 1, \ldots, 4, k = 1, 2,$ is bounded by $\left\|d_{aik}\left(\bar{x}_4\right)\right\| < d_{aikU}$, where d_{aikU} is an unknown constant.

Assumption 4: The inverses of $g_i, \forall i = 2, 4,$ matrices in (3) are positive definite.

Assumption 5: The desired trajectory $x_{1d} = \left[x_{11d}, x_{12d}\right]^T$ is sufficiently smooth.

In backstepping design, we try to reduce the error between actual state and desired state of each subsystem. The tracking error is the error of the first subsystem. Let $e_i = \left[e_{i1}, e_{i2}\right]^T = x_i - x_{id}, i = 1, \ldots, 4$ be the errors.

Step 1:

Let the virtual control law of the first subsystem be

$$x_{2d} = -c_1 e_1 + \dot{x}_{1d} + u_{2dvsc} = \left[x_{21d}, x_{22d}\right]^T,$$

where c_1 is a positive design parameter, u_{2dvsc} is variable structure control law to be designed. From Assumption 3, we have the following inequality

$$\left\|d_{a1j}\left(\bar{x}_4\right)\right\| \le K_{1j}^{*T} \phi_{1j}, \forall j = 1, 2,$$

where $K_{1j}^* = d_{a1jU}$, $\phi_{1j} = 1.$

We let the smooth variable structure control law be in the form $u_{2dvsc} = \left[u_{2dvsc1}, u_{2dvsc2}\right]^T$, where

$$u_{2dvscj} = -\hat{K}_{1j}\bar{\phi}_{1j} = -\hat{K}_{1j}\left(\frac{2}{\pi}\arctan\left(\frac{e_{1j}}{\mu_{1j}}\right)\right),$$

μ_{1j} is a small positive design parameter, $\hat{K}_{1j}$ approximates K_{1j}^* with error given by $\tilde{K}_{1j} = \hat{K}_{1j} - K_{1j}^*$.

The time derivative of the error of the first subsystem becomes

$$\begin{aligned}\dot{e}_1 &= \dot{x}_1 - \dot{x}_{1d} = \left(x_2 + d_{a1}\right) - \dot{x}_{1d} = \left(e_2 + x_{2d} + d_{a1}\right) - \dot{x}_{1d} \\ &= e_2 - c_1 e_1 + u_{2dvsc} + d_{a1}.\end{aligned}$$

Let the weight update law be

$$\dot{\hat{K}}_{1j} = \Gamma_{k1j}[\bar{\phi}_{1j} e_{1j} - \sigma_{k1j}\hat{K}_{1j}],$$

where $\Gamma_{k1j} > 0, \sigma_{k1j} > 0, \forall j = 1, 2.$

Using the following facts

$$\begin{aligned}&2\tilde{K}^T \hat{K} = \left\|\tilde{K}\right\|^2 + \left\|\hat{K}\right\|^2 - \left\|K^*\right\|^2 \ge \left\|\tilde{K}\right\|^2 - \left\|K^*\right\|^2, \\ &0 \le |\alpha| - \alpha\frac{2}{\pi}\arctan\left(\frac{\alpha}{\mu}\right) \le 0.2785\mu, \forall \alpha \in \mathbb{R},\end{aligned} \tag{8}$$

the time derivative of the Lyapunov function

$$V_1 = \frac{1}{2}e_1^T e_1 + \frac{1}{2}\sum_{j=1}^{2}\tilde{K}_{1j}^T \Gamma_{k1j}^{-1}\tilde{K}_{1j},$$

is given by

$$\dot{V}_1 = e_1^T \dot{e}_1 + \sum_{j=1}^{2}\tilde{K}_{1j}^T \Gamma_{k1j}^{-1}\dot{\tilde{K}}_{1j}$$

$$\le e_1^T e_2 - e_1^T c_1 e_1 + \sum_{j=1}^{2}\left(-K_{1j}^{*T}\bar{\phi}_{1j}e_{1j} + K_{1j}^{*T}\phi_{1j}\left|e_{1j}\right| - \tilde{K}_{1j}^T \sigma_{k1j}\hat{K}_{1j}\right)$$

$$\le e_1^T e_2 - e_1^T c_1 e_1 - \sum_{j=1}^{2}\sigma_{k1j}\left\|\tilde{K}_{1j}\right\|^2 / 2 + \xi_1,$$

where

$$\xi_1 = \sum_{j=1}^{2}\left(0.2785\mu_{1j}d_{a1jU} + \sigma_{k1j}\left\|K_{1j}^*\right\|^2 / 2\right).$$

Step 2:

This step is different from the first step because there are unknown functions f_2 and g_2 in this second subsystem. The time-derivative of the error of the second subsystem is given by

$$\dot{e}_2 = \dot{x}_2 - \dot{x}_{2d} = f_2 + g_2\left(x_3 + d_{a2}\right) - \dot{x}_{2d}.$$

Suppose we know f_2 and g_2, and assume there is no disturbance d_{a1} and d_{a2} for now, then we can choose the virtual control input as

$$x_{3d}^* = -e_1 - c_2 e_2 - g_2^{-1}\left(f_2 - \dot{x}_{2d}\right). \tag{9}$$

Using the Lyapunov function $V_2 = e_1^T e_1 / 2 + e_2^T g_2^{-1} e_2 / 2,$ we have $\dot{V}_2 = -c_1 e_1^T e_1 - c_2 e_2^T e_2$ which is negative definite, therefore, the errors e_1 and e_2 converge to zero.

Since we do not know f_2 and g_2, we need to modify the ideal control input x_{3d}^*. From (9), the unknown part is $h_2^*(Z_2) \triangleq g_2(\bar{x}_2)^{-1}[f_2(\bar{x}_2) - \dot{x}_{2d}] = [h_{21}^*, h_{22}^*]^T \in \mathbb{R}^2$, where h_{2j}^* is a scalar-valued continuous function of x_1, x_2, and $\dot{x}_{2jd}$. We proceed by estimating each unknown part using a three-layer neural network. From (4), we have

$$x_{3d}^* = -e_1 - c_2 e_2 - \begin{bmatrix} W_{21}^{*T} S_{21}(V_{21}^{*T} \bar{Z}_{21}) - \varepsilon_{21} \\ W_{22}^{*T} S_{22}(V_{22}^{*T} \bar{Z}_{22}) - \varepsilon_{22} \end{bmatrix}.$$

W_{2j}^* and V_{2j}^* are unknown. Let $\hat{W}_{2j}$ and $\hat{V}_{2j}$ be their estimates and add smooth variable structure control law to handle the uncertainties, we have the virtual control law

$$x_{3d} = -e_1 - c_2 e_2 - \begin{bmatrix} \hat{W}_{21}^T S_{21}(\hat{V}_{21}^T \bar{Z}_{21}) \\ \hat{W}_{22}^T S_{22}(\hat{V}_{22}^T \bar{Z}_{22}) \end{bmatrix} + u_{3dvsc} = [x_{31d}, x_{32d}]^T.$$

From (4), (7), and Assumption 3, we have

$$|d_{u2j}| + |\varepsilon_{2j}| + |d_{a2j}| \le K_{2j}^{*T} \phi_{2j},$$

where

$$K_{2j}^* = \left[\|V_{2j}^*\|_F,\ \|W_{2j}^*\|,\ \|W_{2j}^*\|_1 + \varepsilon_{2jU} + d_{a2jU} \right]^T,$$

$$\phi_{2j} = \left[\|\bar{Z}_{2j} \hat{W}_{2j}^T \hat{S}_{2j}^{'}\|_F,\ \|\hat{S}_{2j}^{'} \hat{V}_{2j}^T \bar{Z}_{2j}\|,\ 1 \right]^T, \forall j = 1, 2.$$

We let the smooth variable structure control law be $u_{3dvsc} = [u_{3dvsc1}, u_{3dvsc2}]^T$, where

$$u_{3dvscj} = -\hat{K}_{2j}{}^T \bar{\phi}_{2j},$$

$$\bar{\phi}_{2j} = \begin{bmatrix} \|\bar{Z}_{2j} \hat{W}_{2j}^T \hat{S}_{2j}^{'}\|_F \dfrac{2}{\pi} \arctan\left(\dfrac{e_{2j}}{\mu_{2j}} \|\bar{Z}_{2j} \hat{W}_{2j}^T \hat{S}_{2j}^{'}\|_F \right) \\ \|\hat{S}_{2j}^{'} \hat{V}_{2j}^T \bar{Z}_{2j}\| \dfrac{2}{\pi} \arctan\left(\dfrac{e_{2j}}{\mu_{2j}} \|\hat{S}_{2j}^{'} \hat{V}_{2j}^T \bar{Z}_{2j}\| \right) \\ \dfrac{2}{\pi} \arctan\left(\dfrac{e_{2j}}{\mu_{2j}} \right) \end{bmatrix}.$$

The time derivative of the error of the second subsystem becomes

$$\dot{e}_2 = g_2 \left\{ \begin{array}{l} e_3 - e_1 - c_2 e_2 \\ + \left[\begin{array}{l} \varepsilon_{21} - \tilde{W}_{21}{}^T (\hat{S}_{21} - \hat{S}_{21}^{'} \hat{V}_{21}{}^T \bar{Z}_{21}) \\ -\hat{W}_{21}{}^T \hat{S}_{21}^{'} \tilde{V}_{21}{}^T \bar{Z}_{21} - d_{u21} - \hat{K}_{21}{}^T \bar{\varphi}_{21} + d_{a21} \\ \hdashline \varepsilon_{22} - \tilde{W}_{22}{}^T (\hat{S}_{22} - \hat{S}_{22}^{'} \hat{V}_{22}{}^T \bar{Z}_{22}) \\ -\hat{W}_{22}{}^T \hat{S}_{22}^{'} \tilde{V}_{22}{}^T \bar{Z}_{22} - d_{u22} - \hat{K}_{22}{}^T \bar{\varphi}_{22} + d_{a22} \end{array} \right] \end{array} \right\}.$$

Let the weight update laws be

$$\dot{\hat{W}}_{2j} = \Gamma_{w2j}[(\hat{S}_{2j} - \hat{S}_{2j}{}^{'} \hat{V}_{2j}{}^T \bar{Z}_{2j}) e_{2j} - \sigma_{w2j} \hat{W}_{2j}],$$

$$\dot{\hat{V}}_{2j} = \Gamma_{v2j}[\bar{Z}_{2j} \hat{W}_{2j}{}^T \hat{S}_{2j}{}^{'} e_{2j} - \sigma_{v2j} \hat{V}_{2j}],$$

$$\dot{\hat{K}}_{2j} = \Gamma_{k2j}[\bar{\phi}_{2j} e_{2j} - \sigma_{k2j} \hat{K}_{2j}],$$

and using the facts (8), and

$$2\tilde{W}^T \hat{W} = \|\tilde{W}\|^2 + \|\hat{W}\|^2 - \|W^*\|^2 \ge \|\tilde{W}\|^2 - \|W^*\|^2,$$

$$2tr\{\tilde{V}^T \hat{V}\} = \|\tilde{V}\|_F^2 + \|\hat{V}\|_F^2 - \|V^*\|_F^2 \ge \|\tilde{V}\|_F^2 - \|V^*\|_F^2,$$

the time derivative of the Lyapunov function

$$V_2 = V_1 + \frac{1}{2} e_2^T g_2^{-1} e_2 + \frac{1}{2} \sum_{j=1}^{2} \Big(\tilde{W}_{2j}^T \Gamma_{w2j}^{-1} \tilde{W}_{2j}$$
$$+ tr\{\tilde{V}_{2j}^T \Gamma_{v2j}^{-1} \tilde{V}_{2j}\} + \tilde{K}_{2j}^T \Gamma_{k2j}^{-1} \tilde{K}_{2j} \Big),$$

derived similar to that in step 1, is given by

$$\dot{V}_2 \le e_2^T e_3 - \sum_{j=1}^{2} \left(\sigma_{w2j} \|\tilde{W}_{2j}\|^2 / 2 + \sigma_{v2j} \|\tilde{V}_{2j}\|_F^2 / 2 \right)$$
$$- \sum_{i=1}^{2} \left(e_i^T c_i e_i - \xi_i \right) - \sum_{i=1}^{2} \sum_{j=1}^{2} \left(\sigma_{kij} \|\tilde{K}_{ij}\|^2 / 2 \right),$$

where

$$\xi_2 = \sum_{j=1}^{2} \Big[0.2785 \mu_{2j} \left(\|V_{2j}^*\|_F + \|W_{2j}^*\| + \|W_{2j}^*\|_1 + \varepsilon_{2jU} + d_{a2jU} \right)$$
$$+ \sigma_{w2j} \|W_{2j}^*\|^2 / 2 + \sigma_{v2j} \|V_{2j}^*\|_F^2 / 2 + \sigma_{k2j} \|K_{2j}^*\|^2 / 2 \Big].$$

Step 3:

This step is similar to step 1. Let the virtual control law be

$$x_{4d} = -e_2 - c_3 e_3 + \dot{x}_{3d} + u_{4dvsc} = [x_{41d}, x_{42d}]^T.$$

We use the smooth variable structure control law as $u_{4dvsc} = [u_{4dvsc1}, u_{4dvsc2}]^T$, where

$$u_{4dvscj} = -\hat{K}_{3j} \bar{\phi}_{3j} = -\hat{K}_{3j} \left(\frac{2}{\pi} \arctan\left(\frac{e_{3j}}{\mu_{3j}} \right) \right).$$

The weight update law is $\dot{\hat{K}}_{3j} = \Gamma_{k3j}[\bar{\phi}_{3j} e_{3j} - \sigma_{k3j} \hat{K}_{3j}]$.

Using a similar derivation to that in step 1, the time derivative of the Lyapunov function

$$V_3 = V_1 + V_2 + \frac{1}{2} e_3^T e_3 + \frac{1}{2} \sum_{j=1}^{2} \tilde{K}_{3j}^T \Gamma_{k3j}^{-1} \tilde{K}_{3j},$$

is given by

$$\dot{V}_3 \le e_3^T e_4 - \sum_{j=1}^{2} \left(\sigma_{w2j} \|\tilde{W}_{2j}\|^2 / 2 + \sigma_{v2j} \|\tilde{V}_{2j}\|_F^2 / 2 \right)$$
$$- \sum_{i=1}^{3} \left(e_i^T c_i e_i - \xi_i \right) - \sum_{i=1}^{3} \sum_{j=1}^{2} \left(\sigma_{kij} \|\tilde{K}_{ij}\|^2 / 2 \right),$$

where $\xi_3 = \sum_{j=1}^{2} \left(0.2785 \mu_{3j} d_{a3jU} + \sigma_{k3j} \|K_{3j}^*\|^2 / 2 \right)$.

Step 4:

This is the last step and is similar to step 2. Let the actual control law be

$$u = -e_3 - c_4 e_4 - \begin{bmatrix} \hat{W}_{41}^T S_{41}(\hat{V}_{41}^T \bar{Z}_{41}) \\ \hat{W}_{42}^T S_{42}(\hat{V}_{42}^T \bar{Z}_{42}) \end{bmatrix} + u_{5dvsc} = [u_1, u_2]^T .$$

The smooth variable structure control law is
$u_{5dvsc} = [u_{5dvsc1}, u_{5dvsc2}]^T$, where

$$u_{5dvscj} = -\hat{K}_{4j}{}^T \bar{\phi}_{4j},$$

$$\bar{\phi}_{4j} = \begin{bmatrix} \left\|\bar{Z}_{4j}\hat{W}_{4j}^T \hat{S}_{4j}^{'}\right\|_F \dfrac{2}{\pi}\arctan\left(\dfrac{e_{4j}}{\mu_{4j}}\left\|\bar{Z}_{4j}\hat{W}_{4j}^T \hat{S}_{4j}^{'}\right\|_F\right) \\ \left\|\hat{S}_{4j}^{'}\hat{V}_{4j}^T \bar{Z}_{4j}\right\| \dfrac{2}{\pi}\arctan\left(\dfrac{e_{4j}}{\mu_{4j}}\left\|\hat{S}_{4j}^{'}\hat{V}_{4j}^T \bar{Z}_{4j}\right\|\right) \\ \dfrac{2}{\pi}\arctan\left(\dfrac{e_{4j}}{\mu_{4j}}\right) \end{bmatrix}.$$

Let the weight update laws be

$$\dot{\hat{W}}_{4j} = \Gamma_{w4j}[(\hat{S}_{4j} - \hat{S}_{4j}{}^{'}\hat{V}_{4j}{}^T \bar{Z}_{4j})e_{4j} - \sigma_{w4j}\hat{W}_{4j}],$$
$$\dot{\hat{V}}_{4j} = \Gamma_{v4j}[\bar{Z}_{4j}\hat{W}_{4j}{}^T \hat{S}_{4j}{}^{'} e_{4j} - \sigma_{v4j}\hat{V}_{4j}],$$
$$\dot{\hat{K}}_{4j} = \Gamma_{k4j}[\bar{\phi}_{4j}e_{4j} - \sigma_{k4j}\hat{K}_{4j}].$$

The time derivative of the Lyapunov function

$$V_4 = V_1 + V_2 + V_3 + \frac{1}{2}e_4^T g_4^{-1} e_4 + \frac{1}{2}\sum_{j=1}^{2}\Big(\tilde{W}_{4j}^T \Gamma_{w4j}^{-1}\tilde{W}_{4j}$$
$$+tr\left\{\tilde{V}_{4j}^T \Gamma_{v4j}^{-1}\tilde{V}_{4j}\right\} + \tilde{K}_{4j}^T \Gamma_{k4j}^{-1}\tilde{K}_{4j}\Big),$$

derived similar to that in step 2, is given by

$$\dot{V}_4 \le -\sum_{j=1}^{2}\left(\sigma_{w2j}\left\|\tilde{W}_{2j}\right\|^2/2 + \sigma_{v2j}\left\|\tilde{V}_{2j}\right\|_F^2/2\right)$$
$$-\sum_{j=1}^{2}\left(\sigma_{w4j}\left\|\tilde{W}_{4j}\right\|^2/2 + \sigma_{v4j}\left\|\tilde{V}_{4j}\right\|_F^2/2\right)$$
$$-\sum_{i=1}^{4}\left(e_i^T c_i e_i - \xi_i\right) - \sum_{i=1}^{4}\sum_{j=1}^{2}\left(\sigma_{kij}\left\|\tilde{K}_{ij}\right\|^2/2\right),$$

where

$$\xi_4 = \sum_{j=1}^{2}\Big[0.2785\mu_{4j}\left(\left\|V_{4j}^*\right\|_F + \left\|W_{4j}^*\right\| + \left\|W_{4j}^*\right\|_1 + \varepsilon_{4jU} + d_{a4jU}\right)$$
$$+\sigma_{w4j}\left\|W_{4j}^*\right\|^2/2 + \sigma_{v4j}\left\|V_{4j}^*\right\|_F^2/2 + \sigma_{k4j}\left\|K_{4j}^*\right\|^2/2\Big].$$

Let

$$\varsigma = \min\left\{\min_{i=1,3}\left\{\frac{c_i}{0.5}\right\}, \min_{j=2,4}\left\{\frac{c_j}{0.5\left\|g_j^{-1}\right\|}\right\}\right\} > 0\ ,\ \ \delta = \sum_{k=1}^{4}\xi_k \ge 0$$

and choose

$$\sigma_{wlj} \ge \varsigma\lambda_{\max}\left\{\Gamma_{wlj}^{-1}\right\}, \sigma_{vlj} \ge \varsigma\lambda_{\max}\left\{\Gamma_{vlj}^{-1}\right\},$$
$$\sigma_{kij} \ge \varsigma\lambda_{\max}\left\{\Gamma_{kij}^{-1}\right\};\ \ l = 2,4;\ \ i = 1,\ldots,4;\ \ j = 1,2,$$

we have $\dot{V}_4 \le -\varsigma V_4 + \delta.$

From this point on, you can use a standard nonlinear analysis technique given, for example, in [16] to conclude that all error trajectories are globally uniformly ultimately bounded. The ultimate bound, time the trajectories enter the bound, and all-time exponential-decay upper bound can also be found, but are omitted here.

5. EXPERIMENTAL RESULTS

There are 4 neural networks; each has 3 hidden nodes. Inputs to each neural network are

$$\bar{Z}_{21} = \{x_{11}, x_{12}, x_{21}, x_{22}, \dot{x}_{21d}, 1\},$$
$$\bar{Z}_{22} = \{x_{11}, x_{12}, x_{21}, x_{22}, \dot{x}_{22d}, 1\},$$
$$\bar{Z}_{41} = \{x_{11}, x_{12}, x_{21}, x_{22}, x_{31}, x_{32}, x_{41}, x_{42}, \dot{x}_{41d}, 1\},$$
$$\bar{Z}_{42} = \{x_{11}, x_{12}, x_{21}, x_{22}, x_{31}, x_{32}, x_{41}, x_{42}, \dot{x}_{42d}, 1\}.$$

Neural network and controller design parameters are as follows:

$$\Gamma_{wij} = \Gamma_{vij} = \Gamma_{kij} = 0.0001, c_i = 5,$$
$$\sigma_{wij} = \sigma_{vij} = \sigma_{kij} = 0.1, \mu = 1.$$

All initial values are set to zeros. Sampling period is 10 ms. The desired trajectory is obtained from passing square wave signal of amplitude 3 and 40-second period into the filter $1/(s+2)^3$.

Experimental results are given in Fig. 5. The control system achieves good overall tracking performance as can be seen from the results in parts (a) and (b). Both link angular positions θ_1 and θ_2 are able to follow their desired trajectories quite closely. Parts (c) to (f) show estimated values of the unknown functions. Parts (g) and (h) are control inputs to the two current amplifiers. Their values can be converted to voltage by multiplying with $10/2^{16}/2$.

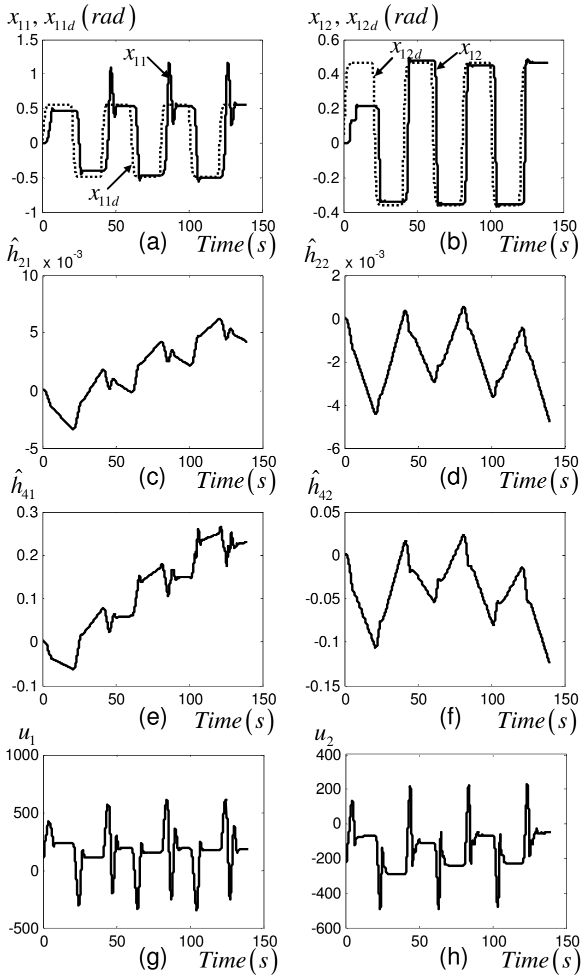

Fig. 5. Experimental results in 140 seconds. (a) θ_1 versus its desired trajectory θ_{1d}. (b) θ_2 versus its desired trajectory θ_{2d}. (c) Estimated function $\hat{h}_{21}$. (d) Estimated function $\hat{h}_{22}$. (e) Estimated function $\hat{h}_{41}$. (f) Estimated function $\hat{h}_{42}$. (g) Control input u_1. (h) Control input u_2.

6. CONCLUSION

The controller achieves good tracking performance. However, there are some interesting questions left as future work. First, the controller is designed based on the assumption that the actual robot is in the nonlinear form (3). The fact that the actual robot may not be exactly in this form may degrade the controller performance. Second, how will the control system handle time-varying case, for example, the change in payload?

REFERENCES

[1] L. M. Sweet and M. C. Good, "Re-definition of the robot motion control problem: effects of plant dynamics drive system constraints, and user requirements," *Proc. of 23rd IEEE Conf. on Decision and Control*, Las Vegas, NV, 1984, pp. 724-731.

[2] M. W. Spong, "Modeling and control of elastic joint robots," *Trans. ASME J. Dynamic Systems, Measurement and Control,* vol. 109, no. 4, pp. 310-319, 1987.

[3] S. Nicosia, P. Tomei, and A. Tornambe, "A nonlinear observer for elastic robots," *IEEE J. Robot. Automat.,* vol. 4, no. 1, pp. 45-52, 1988.

[4] S. S. Ge, "Adaptive control design for flexible joint manipulators," *Automatica,* vol. 32, no. 2, pp. 273-278, 1996.

[5] S. S. Ge, T. H. Lee, and C. J. Harris, *Adaptive Neural Network Control of Robotic Manipulators.* Singapore: World Scientific Publishing, 1998, ch. 7.

[6] M. Spong and M. Vidyasagar, *Robot Dynamics and Control.* New York: Wiley, 1989.

[7] A, De Luca and P. Lucibello, "A general algorithm for dynamic feedback linearization of robots with elastic joints," *Proc. of 1998 IEEE Int. Conf. on Robotics and Automation*, Belgium, pp. 504-510.

[8] B. Brogliato, R. Ortega, and R. Lozano, "Global tracking controllers for flexible-joint manipulators: a comparative study," *Automatica,* vol. 31, no. 7, pp. 941-956, 1995.

[9] A. C. Huang and Y. C. Chen, "Adaptive sliding control for single-link flexible-joint robot with mismatched uncertainties," *IEEE Trans. Contr. Syst. Technol.,* vol. 12, no. 5, pp. 770-775, 2004.

[10] C. W. Park, "Robust stable fuzzy control via fuzzy modeling and feedback linearization with its applications to controlling uncertain single-link flexible joint manipulators," *Journal of Intelligent and Robotic Systems,* vol. 39, pp. 131-147, 2004.

[11] B. Subudhi and A. S. Morris, "Singular perturbation approach to trajectory tracking of flexible robot with joint elasticity," *Int. Journal of Systems Science,* vol. 34, no. 3, pp. 167-179, 2003.

[12] A. A. Schaffer and G. Hirzinger, "A globally stable state feedback controller for flexible joint robots," *Advanced Robotics,* vol. 15, no. 8, pp. 799-814, 2001.

[13] K. I. Funahashi, "On the approximate realization of continuous mappings by neural networks," *Neural Networks*, vol. 2, pp. 183-192, 1989.

[14] A. R. Barron, "Universal approximation bounds for superpositions of a sigmoid function," *IEEE Trans. Inform. Theory,* vol. 39, no. 3, pp. 930-945, 1993.

[15] S. S. Ge, C. C. Hang, T. H. Lee, and T. Zhang, *Stable Adaptive Neural Network Control*. The Netherlands: Kluwer, 2002.

[16] J. T. Spooner, M. Maggiore, R. Ordonez and K. M. Passino, *Stable Adaptive Control and Estimation for Nonlinear Systems*. New York: Wiley Interscience, 2002, ch. 2.